Papillomavirus Research 1 (2015) 74–89

Contents lists available at ScienceDirect

Papillomavirus Research

journal homepage: www.elsevier.com/locate/pvr

Involvement of nucleophosmin (NPM1/B23) in assembly of infectious HPV16 capsids

Patricia M. Day*, Cynthia D. Thompson, Yuk Ying Pang, Douglas R. Lowy, John T. Schiller

Laboratory of Cellular Oncology, NCI, NIH, Bethesda, MD 20892, USA

ARTICLE INFO

Article history:
Received 4 May 2015
Received in revised form
1 June 2015
Accepted 5 June 2015
Available online 25 June 2015

Keywords:
HPV16
Capsid
Assembly
NPM1
B23
Nucleophosmin

ABSTRACT

We report that during assembly of HPV16 pseudovirus (PsV) the minor capsid protein, L2, interacts with the host nucleolar protein nucleophosmin (NPM1/B23). Exogenously-expressed L2 colocalized with NPM1, a complex containing both proteins, could be immunoprecipitated, and L2 could redirect to the nucleus NPM1 that was pharmacologically or genetically restricted to the cytoplasm. Coexpression of the major capsid protein, L1, prevented both the colocalization and the biochemical association, and L1 pentamers could displace L2 from L2/NPM1 complexes attached to a nuclear matrix. HPV16 PsV that was produced in a cell line with reduced NPM1 levels had significantly lower infectivity compared to PsV produced in the parental cell line, although the PsV preparations had comparable L1 and L2 ratios and levels of encapsidated DNA. The PsV produced in NPM1-deficient cells showed increased trypsin sensitivity and exhibited decreased L2 levels during endocytosis. These results suggest a critical role for NPM1 in establishing the correct interactions between L2 and L1 during HPV capsid assembly. A decrease in cellular levels of NPM1 results in the formation of seemingly normal, but unstable, capsids that result in a premature loss of L2, thus inhibiting successful infection. No role for NPM1 in HPV infectious entry was found.

1. Introduction

Papillomaviruses (PV) comprise a large family of non-enveloped DNA viruses that can cause epithelial tumors of the skin and mucous membranes. The replication of PV is intimately linked to the differentiation program of the host epithelia with progeny virions only being produced in the terminally differentiated outer layers [1]. This complicated life cycle prevents the ready analysis of some aspects of PV biology, including assembly. The PV pseudovirus (PsV) system was developed to allow the generation of large quantities of high quality, homogeneous PV capsids that can express an encapsidated marker pseudogenome [2]. PsV are produced in 293TT cells by trans expression of the two PV capsid protein genes in conjunction with the marker plasmid, leading to the formation of PsV by nuclear assembly of the capsid and its packaging the marker pseudogenome. Purified PsV have sufficient homogeneity to enable cryo EM analysis and structure reconstruction [3]. The icosahedral PsV particles are indistinguishable from authentic PV in both structural appearance and disulfide linkages, and have been employed to identify key early steps in the PV life cycle that occur at the plasma membrane and in the cytoplasm and nucleus (reviewed in [4,5]). This in vitro PsV system should also provide an experimentally tractable approach for obtaining insight into essential processes during the nuclear assembly of infectious PV capsids.

The PV protein shell consists of only two proteins: the major capsid protein, L1, and the minor capsid protein, L2. L1 has the capability of self-assembling into virus like particles (VLPs) which, like PsV, resemble authentic capsids morphologically and immunologically [6], and are the basis for the current HPV vaccines [7]. Therefore, L2 is considered dispensable for the gross capsid assembly process. Although examination of BPV1 assembly in cultured cells revealed the L2-dependent nucleation of assembling capsids at the ND10 nuclear subdomain [8], this precise localization was found to be not critical for assembly of HPV31 [9]. Additionally, for some PV types, including HPV16, L2 itself is not essential for encapsidation of the marker pseudogenome during capsid production [2]. However, L2 is essential for the efficient transduction of the marker plasmid during infection by PsV and by authentic PV virions.

L2 has multiple critical roles during infectious viral entry, such as guiding the encapsidated viral genome through the endosomal system and trans-Golgi network to ND10 in the nucleus, where efficient transcription can occur [10–12].

* Corresponding author.
E-mail address: pmd@nih.gov (P.M. Day).

http://dx.doi.org/10.1016/j.pvr.2015.06.005

The ability of the L1/L2 capsid to orchestrate the stepwise uncoating process and release of the L2–genome complex in the host cell depends on the correct assembly of the virus capsid in the cells that produce the infectious PsV. It is likely that host chaperone proteins are recruited by the assembling virion to mediate this process, however little about these potentially critical interactions has been described.

Nucleophosmin (NPM1/B23) is an abundant nuclear phosphoprotein that resides predominantly in the nucleolus. It is involved in multiple cellular processes, including DNA–histone formation, nucleosome assembly, and biogenesis of ribosomal RNA and DNA repair. Increasing evidence has also implicated NPM1 involvement in other diverse viral processes within the nucleus (reviewed in [13]). Here, we report on the role of NPM1 in HPV16 virion assembly and infection, which we investigated because a yeast two-hybrid screen identified an interaction between NPM1 and L2. We find that although NPM1 expression in the target cell is dispensable for HPV16 infection, it plays a critical role during the production phase of the HPV16 lifecycle, in that it interacts with L2 to promote assembly of conformationally correct infectious capsids.

2. Materials and methods

2.1. Yeast two-Hybrid screen

The two-hybrid screen was done through a contract with Myriad Genetics and the NCI using the Center for Cancer Research core facilities. This automated process uses ProNet technology for the large-scale identification of protein-protein interactions based on nuclear yeast two-hybrid methodology as previously described in detail {Nguyen 2008}. HPV16 L2 amino acids 13–474 was used as a bait protein. NPM1 was found to be a strongly interacting prey within a breast cancer/prostate cancer-derived library.

2.2. Cell lines

HeLa, HaCaT and 293 TT cell lines were cultured in DMEM media supplemented with 10% fetal bovine serum (FBS) and penicillin/streptomycin (P/S). FD11 cells and CHOΔfurin cells, obtained from Steven Leppla (NIAID, NIH) and David Fitzgerald (NCI, NIH), respectively, were propagated in DMEM/FBS, P/S and 10 mM proline. NPM1-depleted cell lines were generated by transduction of 293TT cells with lentivirus particles containing a shRNA specifically targeted to NPM1 (TRCN0000062270, Sigma-Aldrich). 293TT cells were plated at 5×10^5 per well in a 12 well plate. Following overnight adherence 10 μl of lentivirus stock and 5 μg/ml polybrene were added to the culture. The following day cells were seeded to a 100 mm plate and supplemented with 2.5 μg/ml puromycin 24 h later. The selection was continuously maintained during cell line expansion and culture. Twenty puromycin-resistant colonies were expanded and analyzed for NPM1 mRNA levels by quantitative PCR (primer set VHPS-6294, RealTimePrimers.com). Western blot quantification of NPM1 protein levels was performed for the three clones exhibiting the lowest NPM1 mRNA levels. Lysate from 1×10^5 cells was analyzed using mouse anti-NPM1 (32–5200, Invitrogen) for detection.

2.3. Antibodies

The rabbit and rat polyclonal antisera recognizing HPV16 L1 capsids were previously described [14,15], as was the polyclonal rabbit antiserum against full length L2 [16], the $11-88 \times 5$ L2 epitopes [17] and the anti-L2 monoclonal antibodies, RG-1 (L2 amino acids 17–36) [18] and L2K-1 (L2 amino acids 64–81) [19]. The Camvir-1 antibody (Abcam) was used to detect HPV16 L1 on Western blots. Nucleoli were detected with clone AE3 that has been widely used to stain specifically the nucleolus (Leinco Technologies). NPM1 antibodies utilized were 32–5200 (Invitrogen) for immunoprecipitation and Western blots and H-106 (Santa Cruz) and AF5205 (R&D Systems) for immunofluorescent localization. The anti-LAMP-1 monoclonal antibody (H4A3) developed by August and Hildreth was obtained from the Developmental Studies Hybridoma Bank developed under the auspices of NICHD and maintained by the Department of Biological Sciences at the University of Iowa [20].

2.4. NPM1 expression plasmids

The NPM1 expression construct pEGFP-C2-flag-NPM was kindly provided by Xin Wei Wang (NCI, NIH) [21]. A 4 basepair insertion (TCTG) at nucleotide position 865 corresponding to NPM1 mutant A genotype [22] was generated with the Quikchange XL (Agilent Technologies) using the primers 5′ gctattcaagatctctgtctggcagtggaggaag 3′ and 5′ cttcctccactgccagacagagatcttgaatagc 3′.

2.5. Pseudovirus production

PsV preparations were produced according to the protocol published on the laboratory website (http://home.ccr.cancer.gov/lco/plasmids.asp). Briefly 293TT cells were transfected with the bicistronic plasmid encoding HPV16 L1 and L2 proteins (p16sheLL) or a carboxyl HA-tagged L2 (p16shellCHA), together with a reporter gene plasmid encoding GFP (p8fwB). Assembled particles were released by detergent lysis, matured in the presence of 25 mM ammonium sulfate and purified by ultracentrifugation through an Optiprep step gradient [23]. Disulfide cross-linking to assess PsV maturation was performed as previously described [23]. Briefly, 10 ng of PsV was alkylated by treatment with 10 mM N-ethylmaleimide (NEM, Pierce) in 10 mM sodium phosphate for 10 min at room temperature. The samples were then incubated in gel loading dye containing 10 mM NEM for 10 min at room temperature followed by 10 min at 65 °C. The samples were electrophoresed through a 3–8% Tris-Acetate NuPage gel (Invitrogen) transferred to Immobilon membrane (Millipore). L1 species were detected with the Camvir-1 antibody. L1 pentamers were produced with the L1 assembly mutant C428S. Pentamers were purified on an Optiprep step gradient (46%, 30%, 20%, 15%) by centrifugation at 50,000 rpm for 1 h at 16 °C using an NVT65 rotor. Pentamer content was confirmed by electron microscopy. Purity and L1 content were assessed following protein staining of SDS-Page gels with SimplyBlue SafeStain (Invitrogen). To assess infection, PsV dilutions were added to HaCaT cells that had been grown overnight at a plating density of 8×10^3 cells per well in 96 well plates. The percent of GFP-transduced cells was determined by flow cytometric analysis after a 72 h infection period.

2.6. Immunofluorescent staining

Cells were seeded onto glass No. 01 coverslips in a 24-well plate at a density of 8×10^4/well and cultured overnight. For evaluation of internalized PsV, 20 ng of PsV was added to each well and allowed to bind and internalize for 24 h. For detection of transfected proteins, transfections were performed directly on the plated cells and incubated for an additional 24 h prior to fixation. When indicated, TmPyP4 (Santa Cruz) was added to cultures 4 h post-transfection at a final concentration of 10 μM. Following this incubation cells were fixed in ice cold ethanol containing 15 mM glycine and processed for immunofluorescent staining as previously described [24] followed by inversion onto DAPI-containing mounting solution (Prolong Gold, Molecular Probes).

The method to detect the time-dependent cell surface exposure of L2 epitopes has been previously described [25]. Briefly, PsV were incubated with HaCaT cells for 1 h, unbound virus was removed, and either processed immediately or incubated for an additional 4 h. Antibody incubations were performed in the cold for 1 h with rocking. Following incubation with the secondary antibody cells were fixed with 2% paraformaldehyde for 20 min at room temperature. Cells were washed three times with PBS/200 mM glycine and inverted onto DAPI-containing mounting solution (Prolong Gold, Molecular Probes). All images were acquired with a Zeiss 780 confocal system interfaced with a Zeiss Axiovert 100 M microscope. In Fig. 9, panels J–L are surface-rendered images processed with Imaris software. Images were collated with Adobe Photoshop software.

2.7. Electron microscopy

100 ng of PsV preparation was applied to a carbon film grid (CF300-Cu, Fisher Scientific) and stained with freshly filtered 1% uranyl acetate. Samples were imaged with an FEI Tecnai T12 transmission electron microscope.

2.8. Immunoprecipitation

293TT cells were transfected with either the bicistronic expression plasmid, p16sheLL, to express both HPV16 L1 and L2 or the plasmid pul to express only HPV16 L2. After 24 h, cells were lysed in immunoprecipitation buffer (50 mM Tris–HCl pH 8.0, 100 mM NaCl, 50 mM NaF, 0.5% NP-40 and 0.1% SDS containing complete protease inhibitor cocktail (Roche)) for 20 min on ice. Cellular debris was removed by centrifugation. Lysates were incubated with rabbit anti-NPM1 antiserum (Santa Cruz) and protein A/G sepharose (Pierce) overnight in the cold with rocking. Immunoprecipitated complexes were collected by centrifugation and washed 4 times in immunoprecipitation buffer. The remaining complexes were boiled in SDS PAGE sample buffer and resolved on a 10% NuPage gel (Invitrogen) and transferred to an Immobilon membrane (Millipore).

2.9. Trypsin stability of capsids

To determine sensitivity to trypsin digestion, 10 μl PsV (500 ng) was incubated with 10 μl of 0.05% trypsin at 37 °C for the time indicated. Following the digestion period, 4 μl of the PsV mixture was processed for L1 detection and 16 μl was processed for L2 detection. Samples were boiled in SDS PAGE sample buffer and resolved on a 10% NuPage gel (Invitrogen) and transferred to an Immobilon membrane (Millipore). L1 was detected with Camvir-1 and L2 was detected with the rabbit anti-full length L2 antiserum.

2.10. L2 stability on cell surface and ECM

Biochemical detection of L2 on the cell surface was assessed by incubating 15 μl PsV (750 ng) with HaCaT cells that had been plated at a density of 2.5×10^6 in 100 mm plates one day prior. Incubation was performed in 8 ml of conditioned medium from either FD11 or Δfurin cells for 4 h at 37 °C. Following this incubation cells were washed twice with PBS and incubated with 5 μl rabbit anti-HPV16 capsid antiserum in 5 ml PBS containing 2% FBS and 0.1% NaN_3 at 4 °C with gentle rocking. Cells were then washed twice with PBS and lysed in situ with 3 ml NP40 lysis buffer (50 mM Tris–HCl pH 8.0, 150 mM NaCl, 1.0% NP-40 and protease inhibitors) for 15 min at 4 °C with rocking. Lysate was retrieved and cellular debris removed by centrifugation. Immune complexes were isolated by incubation with protein A/G sepharose (Pierce) overnight at 4 °C with rocking. The samples were processed for Western analysis as described above. Alternatively, ECM was prepared from HaCaT cells as previously described [17] and 1 μl PsV (5 ng) incubated overnight at 37 °C with 75 μl of conditioned medium from either FD11 or Δfurin cells. Following this incubation ECM was washed three times with PBS and PsV retrieved by addition of NuPage LDS sample buffer (Invitrogen), boiled and processed for L2 detection by Western analysis.

2.11. Matrix extraction of HeLa cells

Following transfection and TmPyP4 treatment as indicated for each experiment cells were extracted according to the protocol of Staufenbiel and Deppert [26]. Briefly, monolayers were washed with Kern-matrix buffer (KM buffer): 10 mM N-morpholinoethanesulfonic acid; 10 mM NaCl; 1.5 mM $MgCl_2$; 10% glycerol; complete protease inhibitor cocktail. The first extraction was performed for 30 min on ice with KM buffer supplemented with 1% Triton-X100, 1 mM EGTA and 5 mM dithiothreitol. Following this extraction buffer was removed and cells were washed three times with KM buffer. The second extraction was performed for 15 min at 37 °C with KM buffer containing 50 μg/ml DNase I. Buffer was removed and cells were washed three times with KM buffer. The third extraction was performed for 30 min on ice with KM buffer containing 2 M NaCl, 1 mM EGTA and 5 mM DTT. Following this final extraction cells were washed with PBS and either fixed immediately or incubated with L1 pentamers (5 μg/ml in PBS containing 5% FBS and protease inhibitor) for 18 h at 37 °C prior to fixation. Following fixation immunofluorescence was performed as described.

3. Results

3.1. NPM1 and L2 interaction

The PV pseudovirus (PsV) production system can produce predominantly uniform assembled PsV particles that can be viewed as acceptable surrogates of authentic wart-derived particles [10,23,27,28]. To better understand the mechanisms of assembly, we examined the intranuclear localization of HPV16 capsid proteins during PsV assembly when they were co-expressed. We also determined the distribution of L2 when it was expressed without L1, as HPV16 L2 is expressed before L1 during HPV replication in vivo [29,30]. PV L2 proteins have a propensity to accumulate at the nuclear subdomain ND10, as determined by L2 colocalization with the defining ND10 resident, PML. During infectious entry, L2 leads the encapsidated genome to this site, and following its trans expression, L2 is often localized at ND10, at least in in vitro systems [8,10].

Here we found that relatively high expression of HPV16 L2 resulted in a heterogeneous nuclear staining pattern that included, in addition to the defined ND10 localization, a larger, more globular accumulation of L2 or diffusely nuclear L2, as previously demonstrated [31]. As some of the larger accumulations of L2 appeared to be vaguely nucleolar or encircling nucleoli, we also examined whether some L2 might localize to nucleoli. The variety of nuclear distributions is illustrated in the micrograph shown in Fig. 1A. When we examined the L2 localization in conjunction with an antibody specific for nucleoli, many L2-expressing cells were found to contain L2 in this ring-like pattern, shown in red, that encircles nucleoli, shown in green (Fig. 1B). We also examined the nuclear distribution of L2 when co-expressed with L1. 293TT cells were transfected with a bicistronic L1 and L2 expression plasmid to ensure that all the transfected cells express both proteins. In the presence of L1, the distribution of L2 was shifted greatly toward a diffuse nucleoplasmic pattern, and the nucleolar-associated rings were no longer evident (Fig. 1C).

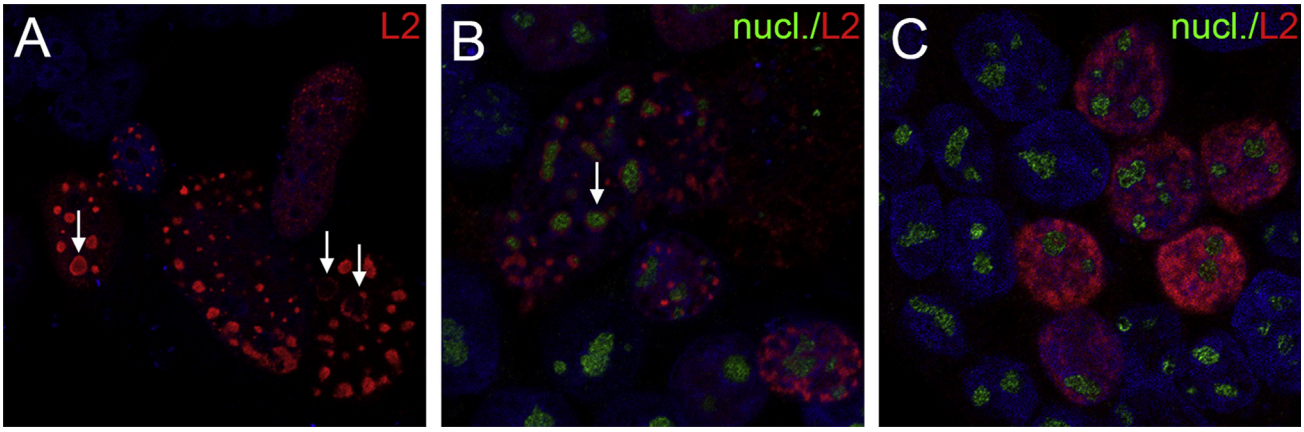

Fig. 1. L2 distribution following transfection. The majority of the L2 protein is located within the nucleus following expression via gene transfection. The variety of distributions, illustrated by the micrograph shown in panel A, includes diffuse nuclear, ND10-like punctate nuclear and a distinct nucleolar-encircling pattern as indicated by the arrows. In panel B we show the L2 staining (red channel) coincident with that of a nucleolar specific antibody (green channel). One example of L2 encircling a nucleolus is indicated by an arrow. Note the L2-positive rings that define the nucleolar boundary. Panel C shows the diffuse nuclear localization of L2 that is observed when co-expressed with L1. Nucleolar staining is shown in green, L2 is shown in the red channel. (For interpretation of the references to color in this figure legend, the reader is referred to the web version of this article.)

We were intrigued by the possibility that a host nucleolar resident protein might be involved in the early steps of HPV16 assembly. Coincident with obtaining the L2 nuclear staining results, Myriad Genetics performed a yeast 2-hybrid analysis for our laboratory using HPV16 L2 amino acids 13–474 as a bait protein. Nucleophosmin (NPM1/B23) was found to be a strongly interacting prey within a breast cancer/prostate cancer-derived cDNA library. NPM1 is an abundant nuclear phosphoprotein that resides predominantly in the nucleolus. It is involved in multiple processes; most interesting to us was its capacity to act as a cellular chaperone. Additionally, it has been demonstrated to participate in assembly of other viruses [32].

To confirm this interaction can occur within mammalian cells, we expressed either HPV16 L2 alone or in conjunction with L1 in 293TT cells by transfection and assessed the ability of an anti-NPM1 antibody to immunoprecipitate L2 or an L2-containing complex. We were able to immunoprecipitate HPV16 L2 in a complex with endogenous NPM1 as shown in Fig. 2, lane 1. However, we were unable to co-immunoprecipitate L2 with NPM1 when L1 and L2 were co-expressed in the cells (Fig. 2, lane 2), although the L2 expression levels in the two conditions were comparable (Fig. 2, lanes 3, 4). The lower band seen in lane 4 is due to slight cross-reactivity of the antibody with the faster migrating L1 protein. Given the reduced interaction in the presence of L1, we did not expect NPM1 to be present in the mature PsV particle preparation; however, we found low, but detectable, amounts of NPM1 associated with the particle (Fig. 2, lane 6). This represents the amount found in 300 ng of purified PsV, whereas lane 5 shows the amount of NPM1 in 100 ng of HeLa cell lysate. The biological significance of this observation is uncertain and may represent NPM1 associated with the minor fraction of malformed or incompletely assembled capsids in the preparations.

Although NPM1 shuttles between the cytoplasm and the nucleus, and within the nucleus it can shift between nucleoplasmic and nucleolar localizations, its steady state localization is predominantly nucleolar [33]. Therefore, we examined the pattern of endogenous NPM1 staining in 293TT cells expressing either only L2 or both capsid proteins. The L2-transfected cells are shown in Fig. 3, panels A–C, with NPM1 staining in the green channel (panels A and C) and L2 staining in the red channel (panels B and C). Varying degrees of colocalization of these two proteins were seen in the L2-expressing cells. Most of the observed colocalization occurred in nucleolar-like structures (indicated by the arrow in panel C), while NPM1 appeared to have shifted from a

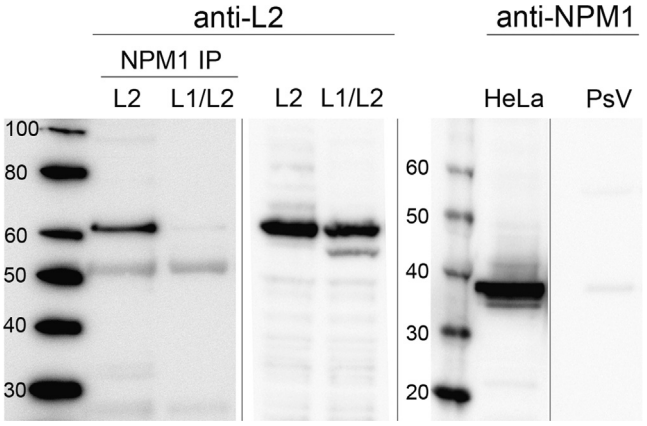

Fig. 2. L2 association with endogenous NPM1. 293TT cells were transfected with either the gene for HPV16 L2 or the bicistronic expression plasmid leading to expression of both capsid proteins. At 24 h post-transfection cell lysates were prepared and immunoprecipitation was performed with a mouse anti-NPM1 antibody and the association of L2 determined by Western analysis with a rabbit anti-L2 antiserum. As labeled, the first lane shows the associated L2 isolated from L2-only expressing cells, whereas the NPM1-associated L2 in the presence of L1 is shown in the second lane. The L2 expression levels in the two conditions were comparable as shown in next two lanes. An anti-NPM1 antibody was used for detection of NPM1 in either 100 ng (total protein) of HeLa cell lysate or 300 ng of purified HPV16 PsV (based on L1 amount).

nucleolar distribution to an ND10-like pattern in a subset of cells (indicated by the arrowhead in panel C). In cells displaying a diffuse nuclear L2 distribution, no change in NPM1 localization was evident (data not shown). It is also important to note that not every cell with either an ND10 or a nucleolar-like L2 expression pattern exhibited a noticeable shift in NPM1 localization. In the untransfected cells, NPM1 was, as expected, found in a nucleolar pattern with varying degrees of cytoplasmic staining. In the cells that were transfected with the bicistronic L1 and L2 expression plasmid, the distribution of L2 was shifted greatly toward a diffuse nucleoplasmic pattern (Fig. 3, panels E and F). Interestingly, NPM1 did not colocalize with L2 under these conditions, and its distribution was similar in the untransfected and transfected populations (Fig. 3 panels D and F). This result is consistent with the previous data shown in Fig. 2, where we demonstrated that co-expression of L1 prevented the ability of L2 to co-immunoprecipitate with NPM1. Therefore, we believe that the predominant NPM1 interaction is with L2 prior to its association with L1 during the PV capsid assembly process.

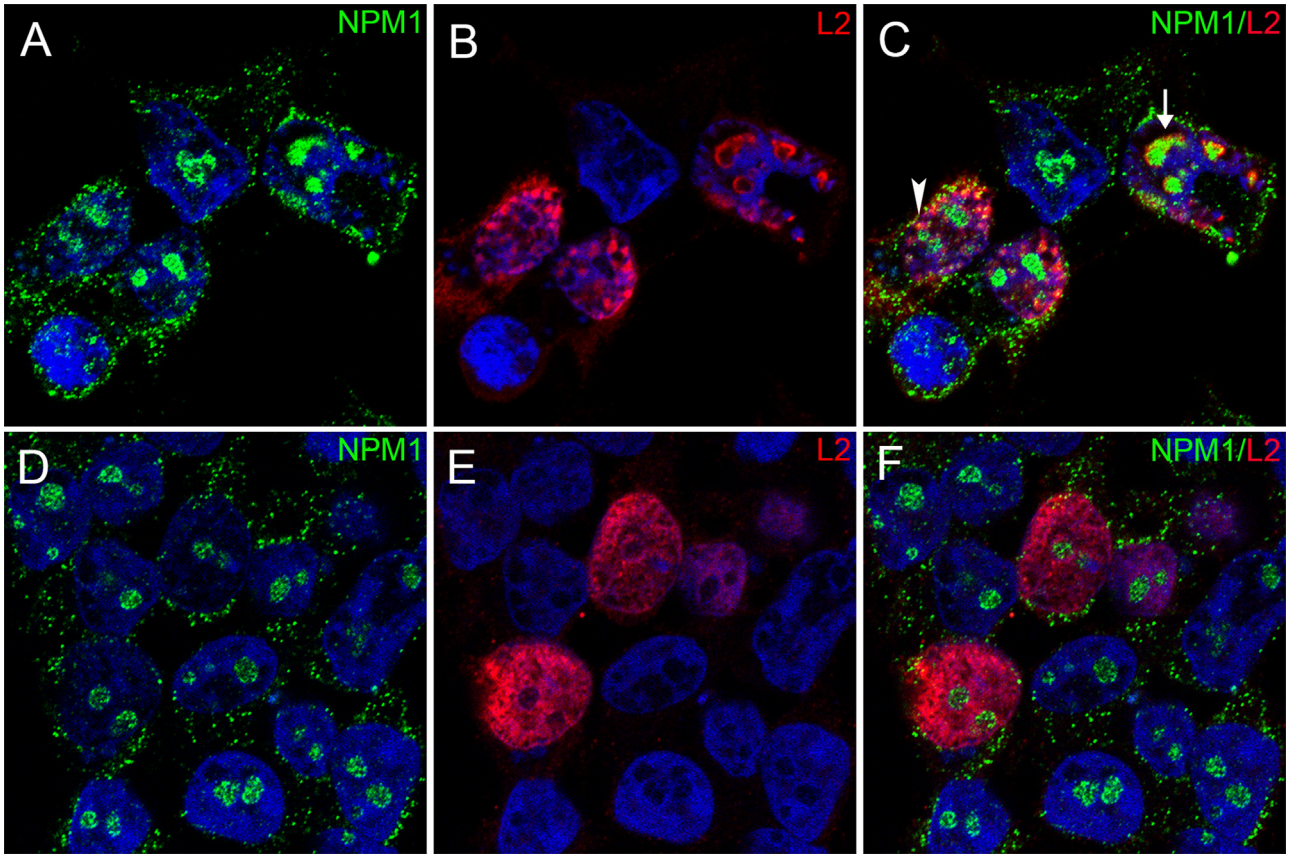

Fig. 3. L2 and NPM1 colocalization. The NPM1 pattern was evaluated in 293TT cells that expressed either L2 (panels A–C) or L1 and L2 (panels D–F). In all cases NPM1 staining is shown in the green channel and L2 staining in the red channel. In the L2-expressing cells, colocalization can be seen in nucleolar-like structures (indicated by arrow in panel C). A more subtle shift of NPM1 into L2+ punctate domains is seen in a subset of cells (indicated by arrowhead in panel C). Neither colocalization nor a shift in NPM1 expression pattern was evident in the cells that expressed both capsid proteins. (For interpretation of the references to color in this figure legend, the reader is referred to the web version of this article.)

3.2. L2 dominantly affects NPM1 localization

These data led us to hypothesize that NPM1 was participating in HPV16 capsid assembly through a transient nuclear interaction with L2. To address this possibility we sought to investigate capsid assembly in the absence of nuclear NPM1. As NPM1 participates in diverse cellular processes, including the crucial control of ribosome biogenesis and centrosome duplication, and deletion of the mouse NPM1 gene results in embryonic lethality [34], we initially decided to pharmacologically diminish intranuclear NPM1 levels instead of reducing total levels by gene silencing techniques.

The C-terminal domain of NPM1 binds to G-quadruplex DNA with high affinity, and this interaction mediates the nucleosomal localization of NPM1. The porphyrin TmPyP4, a G-quadruplex selective ligand, has been shown to prevent association of NPM1 with G-quadruplex DNA; following this treatment, NPM1 is displaced from the nucleoli and primarily accumulates in the cytoplasm [35]. We first analyzed the effect of TmPyP4 treatment on NPM1 localization in HeLa cells. As expected, TmPyP4 treatment for 24 h resulted in the relocalization of NPM1 to the cytoplasm. In Fig. 4, panel A, untreated cells show a clear predominantly nucleolar expression pattern, as we have shown for the 293TT cells. In contrast, in the TmPyP4-treated cells, shown in panel B, almost all of the detectable NPM1 has been relocalized to the cytoplasm. When L2 was expressed under these two conditions, we found that L2 localized well with NPM1 in the untreated cells as expected (Fig. 4, panels C and D), but this was also found to be the case with the TmPyP4-treated cells. As shown in Fig. 4, panels E and F, in the L2-expressing cells, NPM1 relocalized to the nucleus, whereas the untransfected cells showed continued cytoplasmic NPM1 distribution. When we examined the effect of L1 expression on NPM1 localization in these two conditions, we found no colocalization of L1 with NPM1 in either instance, and no effect on the localization of NPM1 in the treated cells (Fig. 4, panels G and H). This result further confirmed the specificity of the L2-NPM1 interaction, but the dominant effect of L2 on the localization of NPM1 precluded the utility of this method for assessing the importance of NPM1 in PsV production. Similar results were seen in 293TT cells (data not shown).

NPM1 has been identified as the most frequently mutated gene in acute myeloid leukemia (AML) [36]. Although multiple NPM1 mutations have been described, they all have the common feature of producing an altered reading frame that leads to the translation of a mutant protein containing four additional C-terminal residues that act as a nuclear export signal (reviewed in [37]). Thus all of the AML mutations result in the cytoplasmic localization of NPM1. Through oligomerization, expression of this mutated form of NPM1 causes the displacement of wild-type NPM1 protein to the cytoplasm. Therefore, we decided to examine the possibility that overexpression of a mutant NPM1 would act functionally as a dominant-negative to allow an evaluation of NPM1-deficient nuclear PsV assembly. We examined the localization of transfected wild-type NPM1 or mutant NPM1 in 293TT cells. Due to the high level of expression from the transfected expression constructs, it was difficult to assess the endogenous NPM1 in these experiments (data not shown). However, nuclear localization of the wild type transfectants (Fig. 5, panel A) and predominantly cytosolic localization of the mutant transfectants was clearly evident (Fig. 5,

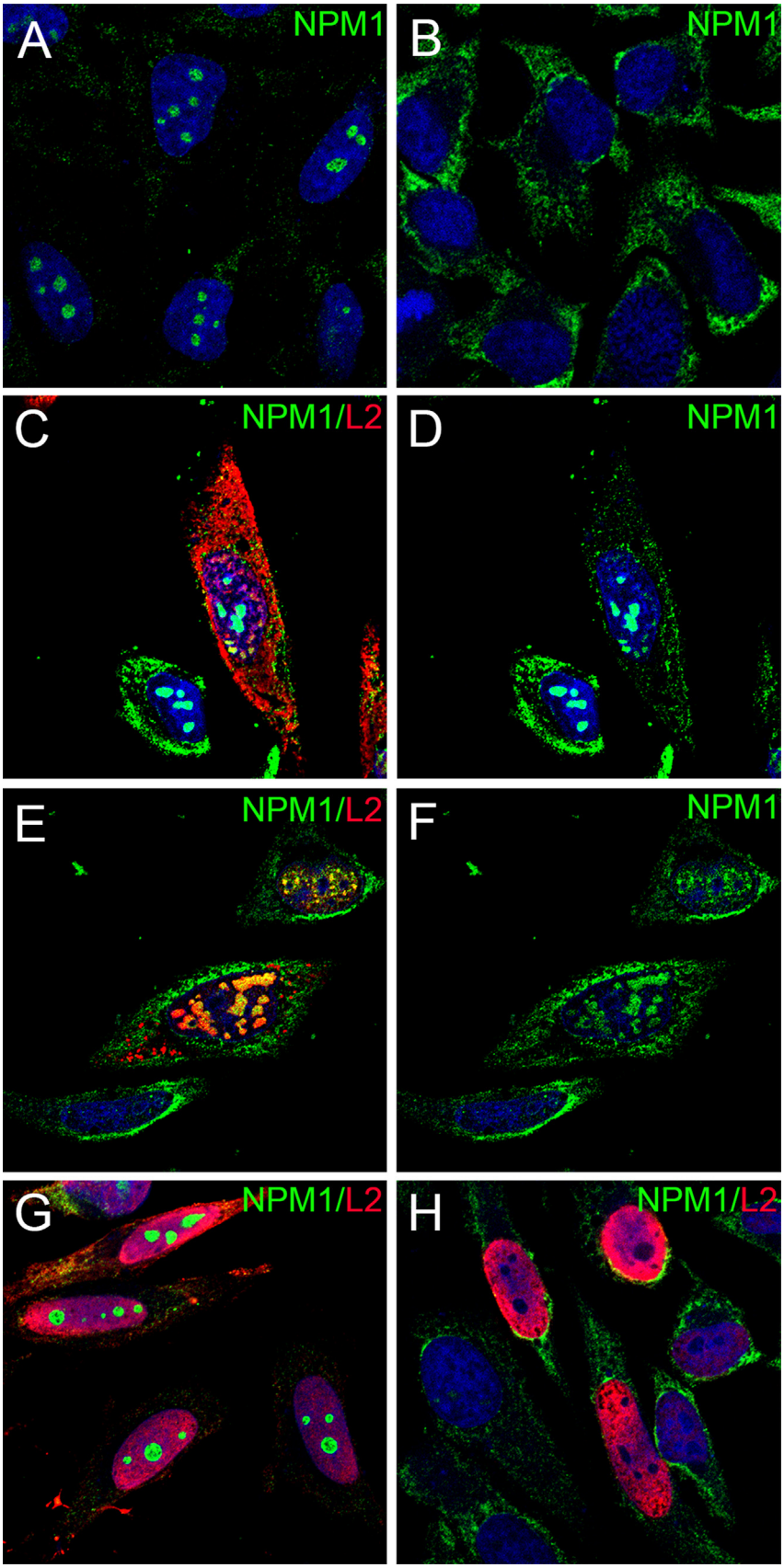

Fig. 4. Effect of TmPyP4 treatment on NPM1 localization. NPM1 localization in untreated HeLa cells is shown in panel A. The cytoplasmic relocalization of NPM1 following overnight treatment with 50 μM TmPyP4 is shown in panel B. Panels C–F show the co-staining of NPM1 (green channel) and L2 (red channel) following transfection with an L2 expression plasmid. Colocalized L2 and NPM1 can be seen in nonnucleolar regions in the untreated conditions (panel C). The NPM1 staining is also shown singly in panel D to enable better visualization of the colocalized regions. Strong nuclear colocalization is seen in both nucleolar and non-nucleolar patterns following TmPyP4 treatment (panel E). Panel F shows only the green channel. Please note the exclusive cytoplasmic NPM1 in the untransfected cell. Expression of both capsid proteins prevents the relocalization of NPM1 as shown in panels G and H. L2 staining is shown in the red channel. NPM1 staining is shown in the green channel. While L2 is diffusely nuclear in both instances, NPM1 is nucleolar in the untreated cells (panel G) and cytoplasmic following TmPyP4 treatment (panel H). (For interpretation of the references to color in this figure legend, the reader is referred to the web version of this article.)

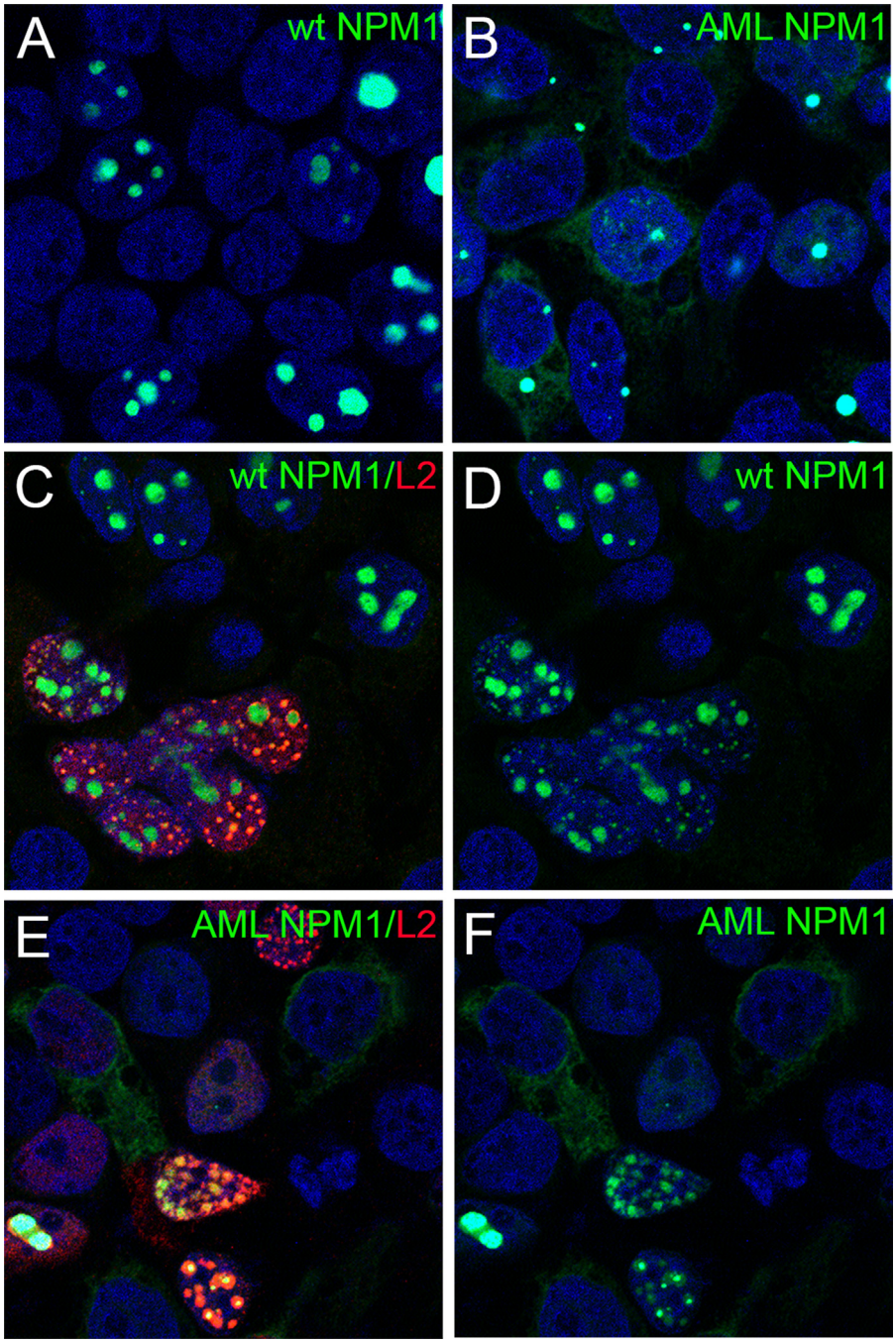

Fig. 5. Localization of overexpressed wild type NPM1 and AML-mutant NPM1. 293TT cells were transfected with either the wild type NPM1 expression construct (panel A) or the AML mutant form (panel B), both are fusion proteins with GFP. Please note that in panel A all NPM1 expression is confined to the nucleus, whereas in panel B fewer nuclear foci are obvious and diffuse cytoplasmic staining is seen. These cells were also co-transfected for L2 expression (panels C–F). L2 staining (red channel) with the wild type NPM1 is shown in panel C. The single channel showing NPM1 staining for this image is shown in panel D. The colocalization of L2 and the mutant NPM1 is shown in panel E, with the NPM1 staining shown singly in panel F. (For interpretation of the references to color in this figure legend, the reader is referred to the web version of this article.)

panel B). When L2 was co-expressed with the wild type NPM1 construct, L2 was seen to be encircling nucleolar NPM1 in addition to some lesser colocalization with NPM1 in punctate nuclear structures (Fig. 5, panels C and D). A similar dominance of L2 localization described above for the TmPyP4 treatment was also evident in this experiment, with L2 causing the nuclear relocalization of mutant NPM1. The colocalization of L2 and the mutant NPM1 was clear in both punctate structures and nucleoli (Fig. 5, panels E and F). The non-L2 expressing cells did not contain nuclear NPM1. Similar results were evident in HeLa cells (data not shown). The results confirm the interaction of NPM1 with L2 and dominant localization activity of L2. Unfortunately, the strength of the L2–NPM1 interaction would prevent the development of this system for analysis of PsV assembled in the absence of nuclear NPM1.

3.3. *L1 pentamers remove L2 from NPM1+ nuclear matrix*

During virus assembly, it has been previously demonstrated that L1 is translocated into the nucleus following capsomer formation in the cytoplasm [29], and these preformed assembly intermediates incorporate L2 and the genome within the nucleus.

Therefore we decided to see if L1 pentameric subunits could displace L2 from NPM1, as this should mimic the biologically relevant assembly cascade, with nuclear L2 and the subsequent introduction of pentamers. To address this scenario, we treated L2-transfected HeLa cells with TmPyP4 to induce strong nuclear colocalization of NPM1 and L2 as shown in Fig. 4. The cells were then subjected to matrix extraction through sequential exposure to detergent, DNase and high salt. It was not possible to use this extraction procedure with the poorly adherent 293TT cells. The matrix extraction of untransfected cells demonstrated that nuclear NPM1 was retained in cells that were not treated with TmPyP4 (Fig. 6, panel A), but the cytoplasmic NPM1 present in the TmPyP4-treated cells was diminished (Fig. 6, panel B). However, in treated cells that had been transfected with L2, NPM1 showed a largely punctate nuclear distribution (Fig. 6, panel C). L2 was also retained following the extraction procedure and colocalized with NPM1 in these prominent nuclear foci (Fig. 6, panel D). Interestingly, in many of these cells it appeared as if L2 formed a "doughnut" encircling NPM1. Following application of L1 pentamers to the skeletal matrix of L2-transfected cells, we observed two distinct distributions of L1 protein association. As seen in Fig. 6, panel E, L1 staining was detected along cell borders and faintly throughout the cell body in subset of cells and in other cells L1 was associated with punctate nuclear foci similar to that observed for L2 and NPM1 (in the presence of L2). It was striking that following application of L1 pentamers the distribution of L2 showed an obvious shift from the characteristic punctate inclusions to a diffuse nuclear distribution in many cells (compare Fig. 6, panels F, no L1, and G, +L1). We quantified the L2 distribution between these two phenotypes in three independent experiments and found that 65–68% of L2+ cells showed a diffuse pattern following L1 pentamer application. This is compared to 26–34% in the cells that were not exposed to exogenous L1. Therefore, exogenous pentamer application to the L2–NPM1 scaffold can mimic the diffuse L2 phenotype, as seen in the presence of L1 following co-expression via transfection, supporting the hypothesis that L1 pentamers directly induce the release of L2 from NPM1-containing nuclear complexes. However, these data do not prove that this scaffold is important for the generation of infectious HPV PsV.

In these experiments, we also observed a distinct loss of L2-associated NPM1 following L1 pentamer application. Although punctate NPM1 was still visible following this treatment it was necessary to adjust the channel gain for acquisition to obtain adequate images. Fig. 6, panel H shows the L2 and NPM1 in cells that were exposed to L1 pentamer, acquired at the identical gain setting as the image shown for non-pentamer exposed cells in Fig. 6, panel D. In Fig. 6, panel I we show the same cells as in panel H, but with the increased gain setting. The L2–NPM1 interaction appeared diminished and fewer L2 "doughnuts" seemed to be formed. To confirm these observations we analyzed Z-stacked series from the various conditions and performed surface rendering on single nuclei. L2, shown in red, is clearly found encircling NPM1, shown in green in the absence of L1 pentamers (Fig. 6, panel J). Fig. 6, panel K shows the same image processing on a nucleus from the L1 pentamer-treated group. It is clear that the NPM1 is more disorganized and not held within the L2 shell. This is consistent with the model that association of L1 pentamers with L2 results in the displacement of NPM1 from L2-containing nuclear foci.

3.4. NPM1 is involved in capsid assembly, but not in HPV PsV infection

Due to the unsuitability of either over-expression of the AML NPM1 mutant or TmPyP4 treatment to investigate NPM1 depletion during HPV PsV assembly, we used an NPM1-specific shRNA to derive NPM1 deficient cell lines from the parental line 293TT. The 293TT cell line was established for the efficient production of PV pseudovirions (PsV), therefore assembly processes are most easily studied in this context. Western blot analysis indicated that the shRNA-derived cell lines have greatly reduced, although still detectable, levels of NPM1 (Fig. 7, panel A). As NPM1 participates in multiple cellular functions critical to survival, the inability to obtain a completely depleted cell line is not surprising. Additionally, the cells tend to revert to higher NPM1 expression over prolonged passage, even with maintained selection pressure (data not shown).

We first evaluated the involvement of NPM1 in the process of HPV infection by comparing the infection potential of the parental 293TT cells with one of the NPM-1 deficient clones, clone 14, which we designated TTC14. The cells were infected with an identical titration series of HPV16 PsV. As seen in Fig. 7, panel B there was no obvious decrease in the infection efficiency of TTC14. Therefore we focused our attention on the hypothesis that NPM1 is involved in HPV16 PsV assembly.

When the ability of the wild type and NPM1-deficient cell lines to produce infectious HPV16 PsV was examined, we found that HPV16 PsV could be produced from every cell line with reduced NPM1 expression, including TTC14. Purified PsV showed typical L1/L2 ratios, histone content (indicative of packaged nucleosomal DNA), and intramolecular L1 disulfide bond formation (data not shown). However, all of the PsV preps showed substantially reduced infectivity compared to PsV produced in parallel in the parental 293TT cells (Fig. 8, panel A).

3.5. NPM1-deficient cells produce defective PsV particles

A larger PsV preparation was prepared and purified from TTC14 cells and, in parallel, from 293TT cells. As before, although the two preparations had similar capsid protein levels, L1/L2 ratio and histone association (Fig. 8, panel B), the infectivity of the PsV preparation assembled in the TTC14 cells was only about 15% that of the PsV produced in parental 293TT cells (data not shown). When negatively stained PsV preparations were analyzed by transmission electron microscopy, no gross structural differences were evident, although this method is sensitive enough to distinguish between immature and mature PsV particles (Fig. 8, panels C and D) [38]. We also confirmed in both PsV preparations that the internal L2 epitope aa 17–36 was inaccessible to the RG-1 monoclonal antibody, which recognizes this epitope and has previously been shown to not immunoprecipitate mature HPV16 PsV under conditions that can immunoprecipitate immature particles and assembly intermediates [25] (Supplemental Fig. S1, panel A). Therefore the TTC14 PsV particles were not grossly defective in particle maturation.

A previous analysis showed that a brief digestion with trypsin had little effect on mature, correctly folded HPV16 PsV particles [38]. To determine if subtle conformational differences could be discerned by trypsin sensitivity, we compared the trypsin sensitivity of TT and TTC14 PsV by digestion for either 30 min or 3 h. Detection of L1 following this treatment showed the appearance of the same tryptic products in both preparations. However, the degree of digestion was higher in the TTC14 preparation, as indicated by the more intense lower bands (Fig. 9, panel A). The examination of L2 showed a more dramatic difference between the two preparations (Fig. 9, panel B), with a distinct digestion product, migrating at approximately 50 kDa, being evident by 30 min in the TTC14 preparation, but not in the TT preparation. At the later time point, L2 was greatly reduced in both preparations, but the decrease was greater in the TTC14 preparation. A longer exposure of the L2 digestion lanes (Fig. 9, panel D) shows the increased laddering of the L2 protein in the TTC14 PsV more clearly. When L1-only PsV were assembled in these two cell lines,

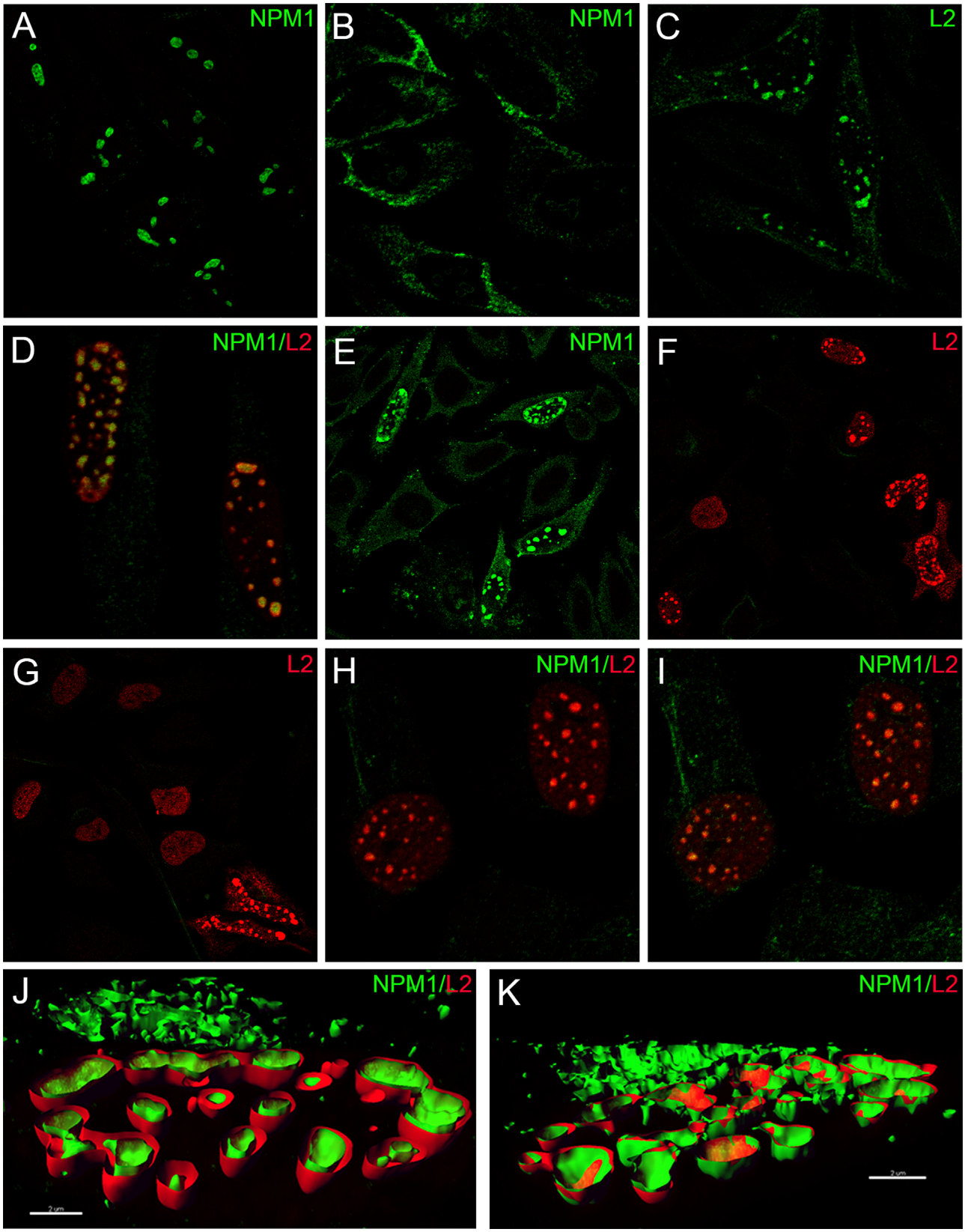

Fig. 6. L1 pentamers disrupt L2–NPM1 association. Matrix extracted HeLa cells are shown in all panels. Panel A shows the NPM1 localization in untreated HeLa cells. All other panels show cells that were treated with TmPyP4 prior to extraction. Panel B shows NPM1 staining in untransfected cells, whereas the staining of L2-expressing cells is shown in Panel C. The colocalization of L2 (red channel) and NPM1 (green channel) is shown in panel D. Please note the apparent localization of L2 around NPM1. Panel E shows the detection of bound L1 following overnight application of L1 pentamers to the extracted matrix from L2-expressing cells. The comparison of panels F and G shows the shift of L2 from a more punctate distribution without L1 pentamers (F) to a more diffuse distribution following L1 pentamer application (G). The detection of NPM1 and L2 in L2-expressing cells following pentamer addition is shown in panels H and I. The conditions for image acquisition for panel H were identical to that for panel D (no pentamers). The green gain was increased in panel I to allow visualization of NPM1. Nuclei from these two conditions analyzed by surface rendering are shown in panels J (no pentamers) and K (+ pentamers). (For interpretation of the references to color in this figure legend, the reader is referred to the web version of this article.)

and compared for trypsin resistance, the differences were less pronounced than seen for the PsV preparations containing both L1 and L2 (Fig. 9, panel C). This observation suggests that most of the reduced trypsin resistance of L1 in the TTC14-produced capsids was L2-dependent.

3.6. Entry of TT and TTC14 PsV

We then determined if there were any obvious differences in the endocytosis and trafficking of the PsV produced from the two cell lines, by allowing PsV to enter HeLa cells for 24 h and examining the localization of the two capsid proteins. For both PsV preparations, L1 showed good colocalization with LAMP-1, indicating successful delivery into the late endosomal/lysosomal compartment, (Fig. 10, compare panel A [TT PsV] with panel B [C14TT PsV]). In contrast, examination of the L2 distribution following endocytosis showed striking differences between the two PsV preparations. For the TT PsV, L2 was localized predominantly in perinuclear accumulations, most likely representing the Golgi complex as previously described [11,12], and additionally in small peripheral vesicles (Fig. 10, panel C). However, L2 from TTC14 PsV was only localized in sparse peripheral vesicles (Fig. 10, panel

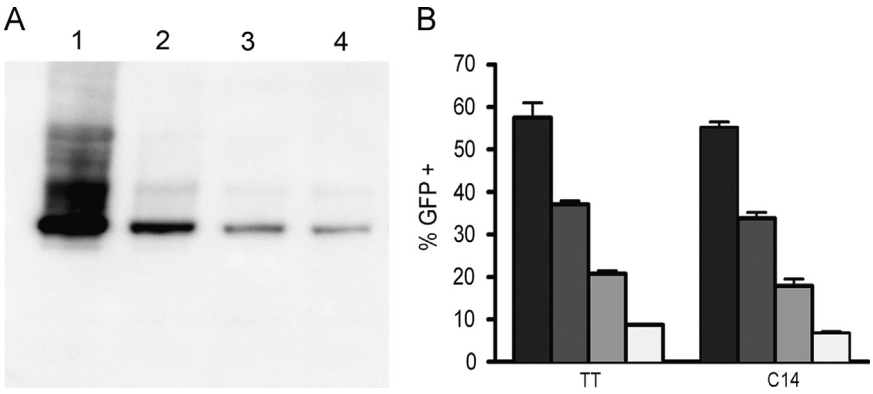

Fig. 7. NPM1-deficient cell lines. NPM1-deficient cell lines were isolated by puromycin selection and assessed for mRNA levels by qPCR (data not shown). Three cell lines were analyzed for NPM1 expression by Western blot analysis (panel A). The parental cell line 293TT cell line is shown in lane 1. Clones C2, C14 and C19 are shown in lanes 2, 3 and 4, respectively. The comparison of HPV16 PsV infection of clone C14 and the parental 293TT cell line is shown in panel B. Infection, in triplicate, with a dilution series of HPV16 PsV containing a GFP reporter plasmid was analyzed by flow cytometry following a 48 h infection period.

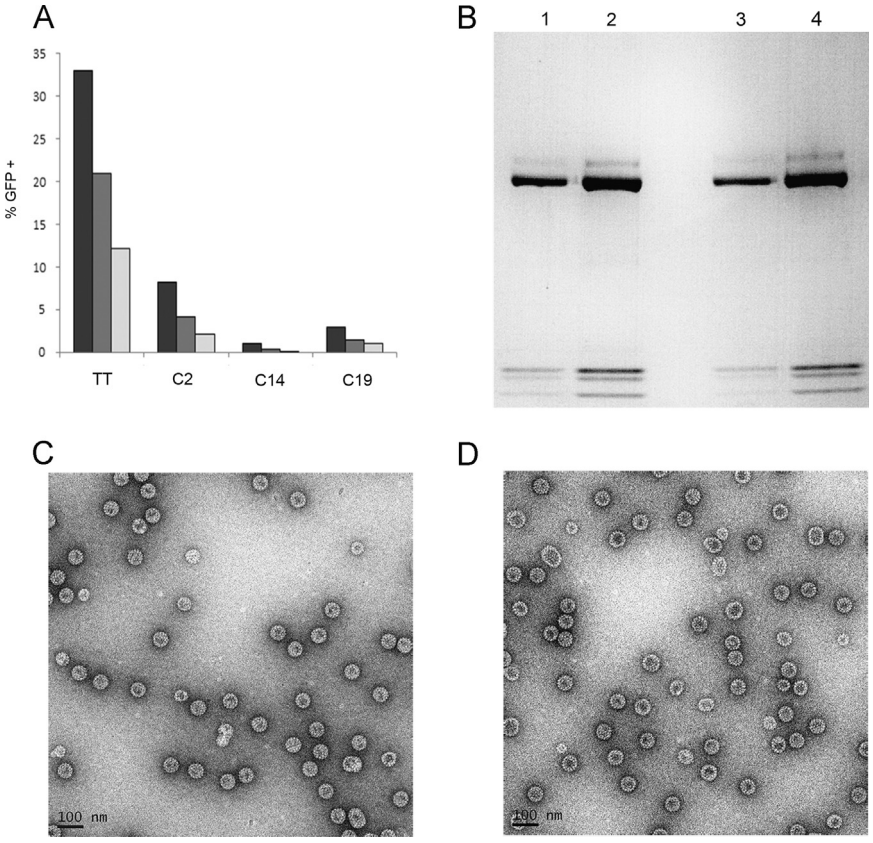

Fig. 8. PsV assembly in NPM-1 deficient cell lines. HPV16 PsVs containing a GFP-reporter plasmid were made in each of the cell lines. Purified PsV was equilibrated by L1 amount and assessed by flow cytometry for infectivity following incubation with HaCaT cells for 72 h. Three dilutions were evaluated (panel A). The infection was reduced by 75–84% with C2 PsV, 97–99% with C14 PsV, and 92–93% with C19 PsV. The protein gel of 2 amounts of PsV from 293TT (lanes 1 and 2) and C14 (lanes 3 and 4) is shown in panel B. The lower bands represent histones present on the packaged DNA. The two upper bands are the capsid proteins. The less abundant L2 migrates slightly more slowly than L1. Electron microscopic analysis of negatively stained 293TT- and C14-produced PsV is shown in panel C and D, respectively.

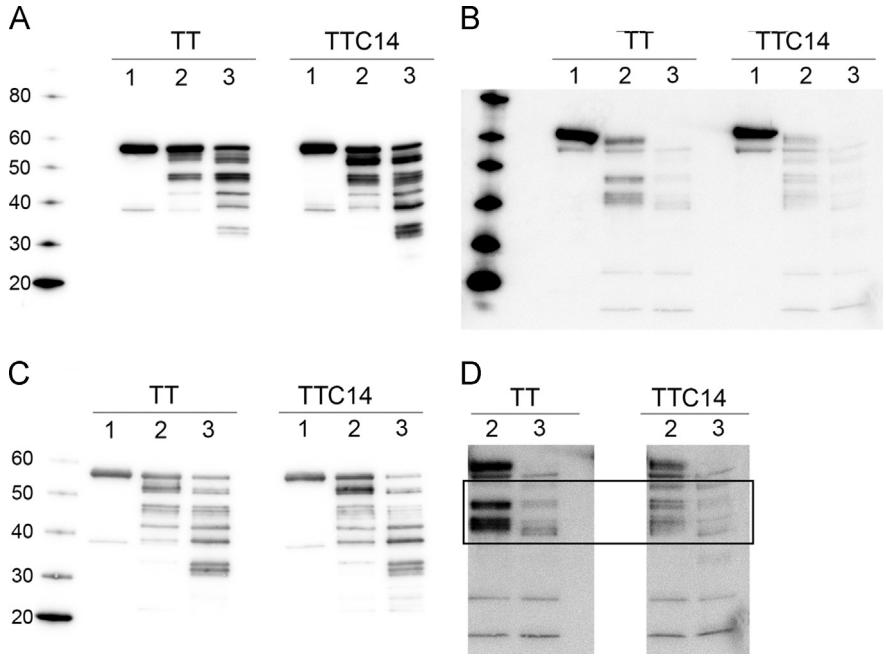

Fig. 9. Trypsin sensitivity of PsV. The trypsin resistance of TT and TTC14 PsV preparations was evaluated. Purified PsVs were incubated with an equal volume of 0.05% trypsin for either 30 min or 3 h and compared to untreated samples by Western blot analysis. Panel A shows the anti-L1 immunoblot. Untreated samples are in lane 1, the 30 min treatment is shown in lane 2, and the 3 h treatment is lane 3. The source of the PsV is indicated above the lanes. Note the increased intensity of the lower bands in the trypsin-treated TTC14 lanes. Panel B shows the detection of L2 following the same treatment regimen. Please note the increase in the number of trypsin digestion products in the TTC14 PsV sample following 30 min incubation and near complete loss of L2 by 3 h. Panel D shows a longer exposure of the same immunoblot to allow greater appreciation of the differences between the PsV preparations. The boxed area encompasses the regions to compare between the two PsV preparations. The untreated lanes were cropped out to prevent visual interference from over-exposure. Panel C shows the anti-L1 blot for the same protocol using L1-only particles prepared from the two cell lines. The differences between the two preparations are less pronounced than that seen with the L2-containing PsV (compare to panel A).

D). Also, the amount of L2 appeared to be less after infection with the TTC14 PsV, possibly due to aberrant trafficking and subsequent degradation or its becoming inaccessible to staining.

During infectious entry, conformational changes allow the exposure of the amino terminus of L2 to cellular proprotein convertases, most notably furin. Furin cleaves the extreme amino terminus (at aa 12 for HPV16) and exposes the N-terminal cross-neutralization epitope to antibodies [39,40]. We previously developed a method to assess this temporal epitope exposure on the surface of cells [25]. To determine if the TTC14 PsV exhibit a deficit in this essential event, we compared L2 epitope exposure for the two PsV preparations. PsV were adsorbed to HaCaT cells for 1 h at 37 °C, and the incubation was either terminated at this point or the cells were washed and reincubated for a 4 h chase period. The amount of PsV binding was determined by anti-L1 staining and the extent of L2 exposure was also measured, using the RG-1 monoclonal antibody. For both PsV preparations, capsid binding at the 1 h time point was readily detected (Fig. 11, panels A and C), and, as expected at this early time point, little L2 antibody binding occurred (Fig. 11, panels B and D), although, we found slightly increased L2 staining with the TTC14 PsV preparation (panel D). As mentioned previously, RG-1 was incapable of recognizing these capsids in solution, as evidenced by its inability to immunoprecipitate TT-derived PsV. Therefore, these results likely indicate a change in conformation that occurs soon after cell interaction, unlike with the TT PsV seen here and previously [25]. Following the longer incubation time, the levels of cell surface L1 were essentially unchanged for the two PsV preparations (Fig. 11, panels E and G). As expected, the capsid conformational changes and furin cleavage that occurred during this chase period allowed antibody access to the L2 17–36 region in the case of the TT-produced PsV (Fig. 10, panel F). In contrast, no signal was evident for the TTC14 PsV (Fig. 11, panel H) at this later time point, despite the slightly higher degree of staining at the 1 h time point. To confirm this result, we also examined the L2 staining with a polyclonal serum that was raised against the 11–88 region of L2, which produced findings similar to RG-1 (data not shown).

3.7. Loss of L2 from cell surface and ECM-bound PsV

Based on the microscopic analyses, we hypothesized that L2 is somehow lost or released from the capsid during infection. The loss or release could occur either during endocytosis, as found in the initial experiment, or at the cell surface, as found in the second experiment. To confirm the L2 loss biochemically, we examined the amount of cell surface L2 following PsV attachment and furin cleavage. After binding the PsV to HaCaT cells for 4 h, the cell surface-associated capsids were immunoprecipitated with an anti-L1 antibody, and L1-associated L2 levels in the immunoprecipitates were determined by Western blot analysis. In the microscopic analysis shown in Fig. 11, only the L2 that has exposed RG-1 epitopes could give a positive antibody signal, whereas in this experiment we would theoretically detect all of the capsid-associated L2. Because of this difference, we also performed the analysis with the addition of exogenous furin to ensure more complete and rapid cleavage of L2, and potentially its loss as well. As shown in Fig. 12, panel A, there was little difference in the L1 protein levels between the TT and TTC14 PsV samples, either with or without exogenous furin. Even in the absence of exogenous furin, there was a subtle decrease in the amount of L2 in the TTC14 preparation compared to the TT PsV, and this difference was magnified in the presence of furin (Fig. 12, panel B). Thus, these results are similar to the microscopic findings. However, the difference in the amount of L2 observed with the biochemical method, which detects all L2 associated with L1 on the cell surface, was smaller than that observed microscopically, which only detected furin-cleaved L2. Ideally, we would determine the L2 loss that occurs during the entire endocytic process, however we were

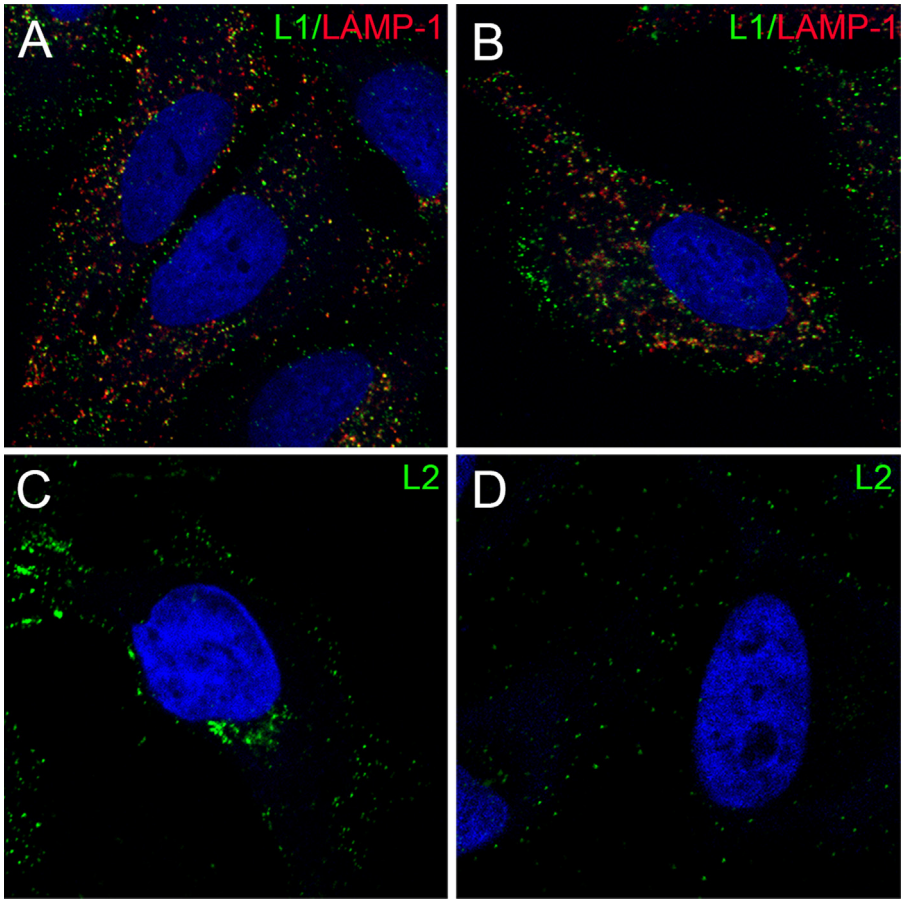

Fig. 10. PsV endocytosis. HeLa cells were infected for 24 h with PsV from either TT cells (panels A and C) or TTC14 cells (panels B and D). Colocalization of L1 (green channel) and the late endosomal/lysosomal marker LAMP-1 (red channel) is shown in panels A and B. The distribution of L2 is shown in panels C and D; note the perinuclear distribution of L2 in panel C. (For interpretation of the references to color in this figure legend, the reader is referred to the web version of this article.)

not able to reliably detect L2 from internalized PsV when we added a reasonable amount of PsV per cell; even a dose of 15,000 capsids per cell was not adequate following an overnight incubation (data not shown).

As an alternative biochemical method, we examined the PsV preparations following attachment to extracellular matrix (ECM) derived from HaCaT cells. HPV16 PsV has been shown to bind well to this matrix, and this interaction allows the necessary conformational changes to the HPV16 capsid that expose the furin cleavage site on the L2 N-terminus [17]. The addition of cell-free exogenous furin to these bound PsV allows furin cleavage to occur on the ECM without any need for host cell interaction. For this experiment, we incubated the two PsV preparations with ECM with or without exogenous furin and evaluated L2 loss. We used PsV that contained a carboxyl-HA tagged L2 protein in order to assess the loss of full length L2 versus the potential clipping of the more amino-terminal epitope that we had examined in the previous experiments. Following the overnight incubation necessary to obtain complete furin digestion of L2, we saw no difference in matrix-bound L1 protein levels between the two PsV and no detectable change in L1 levels due to exposure to furin (Fig. 12, panel C). However, we saw a furin-dependent decrease in the amount of matrix-bound L2 in the TTC14 PsV that was evident with either the anti-HA antibody(Fig. 12, panel D), indicating loss of the entire L2 protein, or antibody L2K-1, which recognizes an epitope within amino acids 64–81 of L2 (Fig. 12, panel E). No loss of L2 was evident in the TT PsV preparations with either antibody. A slightly faster migrating band was evident in both PsV preps in the conditions that were exposed to exogenous furin. This band likely represents detection of the furin-cleaved L2 following the loss of the N-terminal end. The results indicate that L2 is less stably associated with capsids produced in NPM1-deficient cells after they have undergone HPSG-induced conformational changes and furin cleavage.

4. Discussion

The importance of L2 for the generation of infectious PV virions has long been appreciated. Although L2 is not critical for the assembly of the icosahedral capsid, it is necessary for correct delivery of the viral genome into the host cell, and for many HPV types it is also essential for the encapsidation of the genome (reviewed in [41]). What has been little understood is how L2 and the L1 pentamers assemble within the nucleus. L1 protomer to pentameric capsomer assembly occurs in the cytoplasm [29]. Assembled pentamers are then translocated into the nucleus for subsequent association with L2 and the viral genome. A requirement for the chaperone Hsc70 in the nuclear translocation of L2 has also been described [42]. Within the nucleus Hsc70 and the co-chaperone Hsp40 are found in a complex with L2, but are displaced during later assembly processes, as the chaperone proteins are not associated with the fully assembled capsid. It has been suggested that Hsc70 may participate in the incorporation of L2 or genome into the viral capsid. More recently the sumoylation of L2 was demonstrated [43]. This modification was only present in the absence of L1, so it would presumably make an early contribution to the assembly process or L2 localization prior

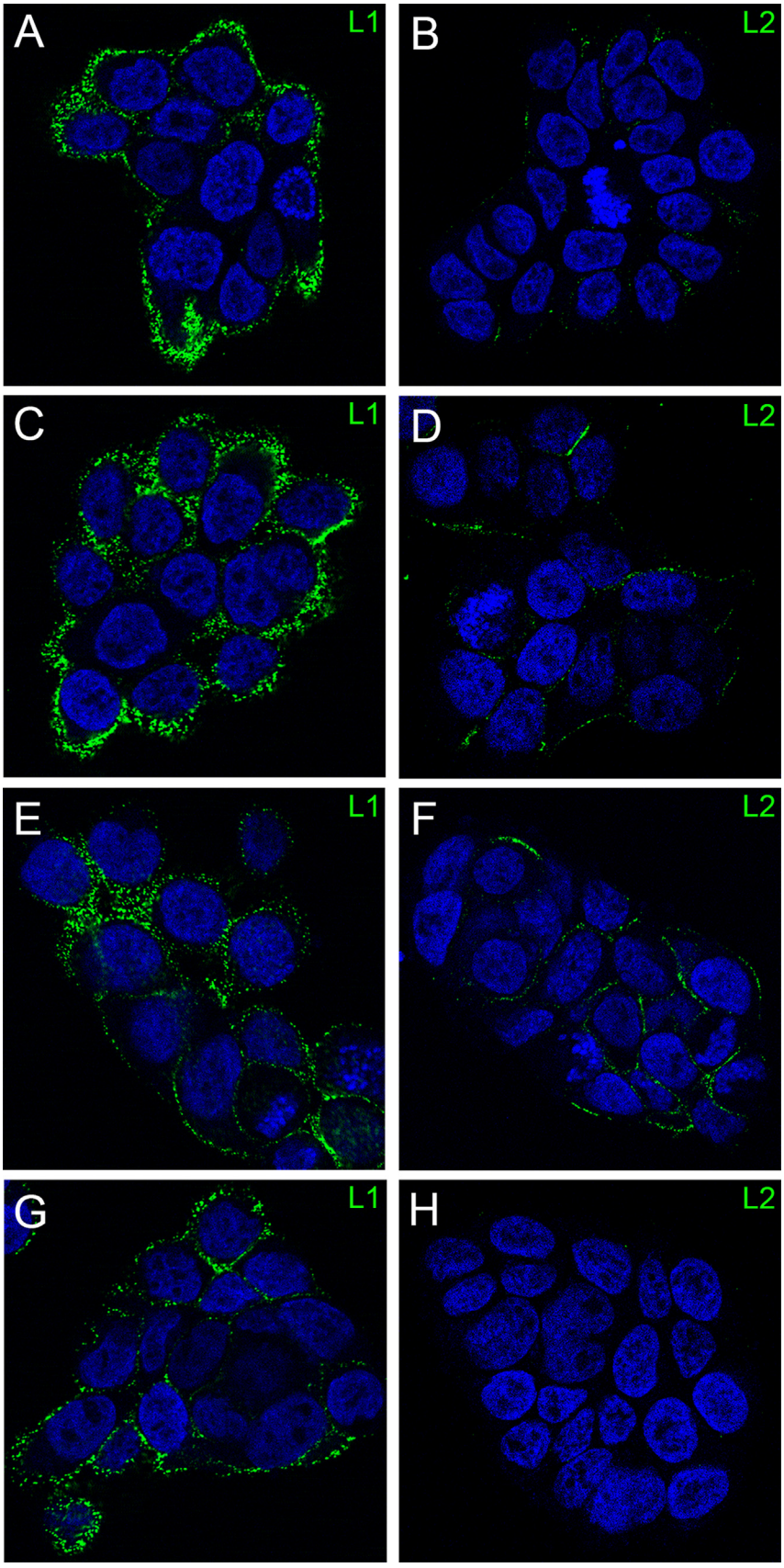

Fig. 11. Detection of cell surface L2. PsVs were allowed to bind to HaCaT cells at 37 °C for 1 h. Cells were washed and stained prior to fixation with either an anti-L1 antiserum or an anti-L2 antibody, RG-1, which recognizes the 17-36 epitope. TT PsV is shown in panels A (L1) and B (L2), while C14 PsV is shown in panels C (L1) and D (L2). Cells were also processed following a 4 h chase period. During this time L1 staining remains constant; panel E shows TT PsV and panel G shows C14 PsV. Increased L2 antibody binding on TT PsV is shown in panel F. The lack of anti-L2 reactivity on C14 PsV is shown in panel H.

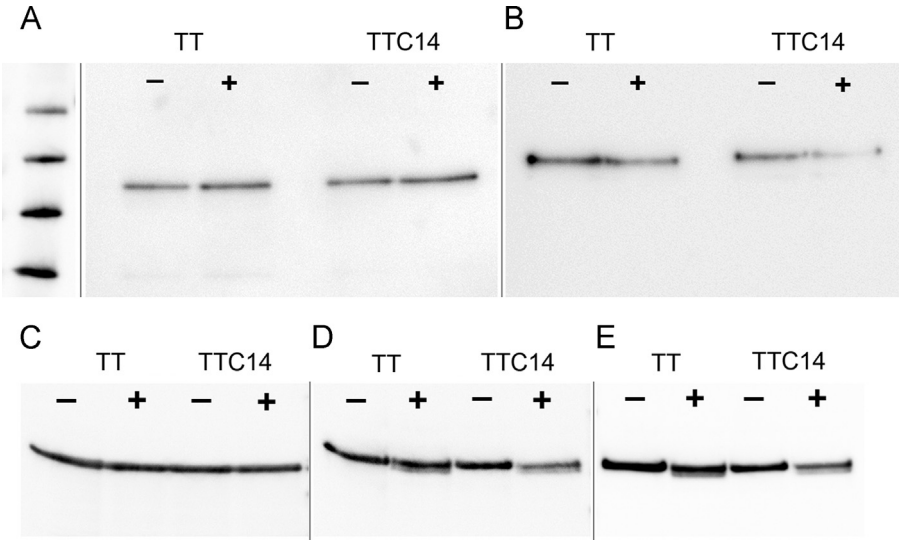

Fig. 12. Biochemical detection of L2 following cell surface or ECM PsV binding. Panels A and B show the immunoblot analysis of PsV associated with the HaCaT cell surface. PsV were bound to HaCaT cells for 4 h at 37 °C either in conditioned medium from either FD11 cells (indicated by – symbol above the lane) or from Δfurin cells (indicated by a + symbol). Cell surface PsV were immunoprecipitated by application of an anti-L1 polyclonal serum prior to cell lysis and analyzed for either L1 (panel A) or L2 (panel B) protein content. Camvir-1 was used for L1 detection and the RG-1 (17–36) antibody was used for L2 detection. Panels C–E show the analysis of PsV bound to HaCaT-derived ECM. PsV containing C-terminally HA-tagged L2 were bound to the ECM for 18 h at 37 °C either in conditioned medium from FD11 cells or Δfurin cells. Panel C shows the detection of L1, panels D and E show the detection of L2 with either anti-HA (panel D) or with L2K-1, a monoclonal antibody reactive against an epitope within amino acids 64–81.

to assembly. Aside from these studies, there has been a dearth of experimental evidence on the host contribution to PV assembly. In the current work, we show that the NPM1/B23, a nucleolar phosphoprotein, plays an important role in this process.

It has become increasingly evident that the nucleolus has diverse functions beyond its initially assigned role in ribosome biogenesis (reviewed in [44]). The composition of nucleoli is dynamic during cell cycle progression and signaling events important during normal growth conditions [45]. They are also greatly affected by conditions of cell stress due to environmental conditions, disease, or viral infection. The ever-growing nucleolar proteome presently contains more than 4500 entries, including an abundance of chaperone proteins, a subset of which has recently been termed nucleolar multitasking proteins (NoMPs) [46]. NoMPs act not only as RNA or protein chaperones, but also contribute fundamentally to nucleolar organization and function. NPM1/B23 has been designated a NoMP due its numerous and far-reaching functions.

To the growing list of NPM1 functions, we would add assembly of infectious HPV16 PsV. Based on the accumulated data, we envision that NPM1 plays an early role in the assembly process. L1 expression prevents or reverses the association between L2 and NPM1, and we have also shown that L1 expression shifts the localization of L2 towards a more nucleoplasmic distribution without an obvious coincident shift in NPM1 localization, whereas in the absence of L1, L2 frequently encircles the nucleoli. NPM1 could act as a chaperone to ensure proper folding of nuclear L2 and/or act as a scaffold to position L2 for proper interaction with L1 pentamers. It is intriguing that NPM1 also possesses a pentameric structure. We can envision an L2–NPM1 complex initiating an assembly scaffold, possibly positioning L2 correctly within a pentameric mold, around which L1 pentamers could accrete, displacing NPM1 during the process. Indeed when we add exogenous pentamers to an L2–NPM1 scaffold on extracted cell matrices, we can visualize the displacement of L2 and diffuse relocalization. Additionally, in the nuclei that continue to bear punctate L2, the interaction with NPM1 appears to be decreased and disrupted. Although low levels of NPM1 are present in mature PsV capsid preparations, this NPM1 may be associated with the small amounts of partially assembled or misassembled capsid structures present, and we doubt that it is functionally significant.

It is unclear if NPM1 functions directly in PV assembly or by recruitment of other chaperones. As L2 modification by Sumo 2/3 could influence protein-protein interactions, we considered the possibility that L2 sumoylation could be involved in L2–NPM1 interactions. However, no differences in L2 association with Sumo 2/3 in the 293TT and C14TT cell lines were detected (data not shown). Also the previously described L2 sumoylation-defective mutant and wild type L2 could interact equally well with NPM1 (data not shown). We similarly found no difference in the nuclear relocalization of Hsc70 in the presence of L2 between the two cell lines (data not shown).

Lack of adequate levels of NPM1 clearly has a negative effect on the production of infectious particles, although there was no obvious defect based on EM analysis, capsid protein ratio and DNA encapsidation. However, although we found no difference in the levels of disulfide bonding within the capsids (Supplemental Fig. S1, panel B), capsid stability was clearly affected as trypsin sensitivity was increased, with an almost complete loss of L2 observed in this in vitro assay. L2 was also lost from the capsid during endocytosis. We further showed that this reduction in L2 could occur at the cell surface following furin cleavage, or subsequent to furin cleavage following ECM attachment. Thus we postulate that NPM1 functions to ensure that L2 is properly folded/positioned in association with the L1 capsid shell such that it remains firmly attached to the capsid after the initial HSPG-induced conformational change and removal of the N-terminus of L2 by furin cleavage. There is evidence for an involvement of Cyclophilin B in mediating L2 conformational changes that allow furin cleavage, as this occurs prior to our observed loss of L2, we do not anticipate the involvement of this host chaperone in the process [47].

Although L2 can clearly associate with endogenous NPM1, which is predominantly nucleolar, it seems that L2 has a greater propensity to interact with non-nucleolar NPM1, as evidenced by the TmPyP4 treatment and NPM1 trans expression experiments. With both methods of NPM1 delocalization, nearly complete nuclear colocalization with L2 could be observed. This is strong

evidence of a specific interaction between the two proteins. The relocalization of cytoplasmic NPM1 was prevented with co-expression of L1, providing further indication of a mutually exclusive L2 interaction. As to why the enhanced interaction with delocalized NPM1 occurs; perhaps only a subset of nuclear NPM1 is available for L2 binding, because of strong mutually exclusive association with other nuclear proteins, whereas following de novo NPM1 synthesis or delocalization of NPM1, L2 can associate with a larger pool of protein. It is also possible that L2 interacts more strongly with monomeric NPM1, which is present in lower amounts than oligomeric NPM1 and is associated with nucleoplasmic accumulation [48].

Other virus proteins, from a broad distribution of virus types, have been demonstrated to interact with NPM1. In some instances, NPM1 affects viral transcription by chaperoning viral proteins to initiate promoter interactions, as is seen with EBV [49]. In other cases, although NPM1 expression is necessary for viral replication and a direct interaction with a viral protein has been determined, the mechanism by which NPM1 promotes infection is not yet understood. This is the case with Japanese Encephalitis Virus and Newcastle disease virus [50,51]. The nucleolus has been described as the site of assembly for AAV2 [52]. However, it is currently unclear which host nucleolar proteins are necessary to complete the assembly reaction for this virus.

Among the reported roles of NPM1 in viral infection, its interaction with adenovirus has the most parallels to what we have observed with HPV16. NPM1 is essential for adenovirus replication in normal cells and has been shown to interact critically with protein V, which is involved in capsid assembly. NPM1 is not incorporated into the fully assembled particle, but is found to be associated with empty particles, suggesting a scaffolding function [32]. No particle formation was detected in normal cells infected with a mutant virus encoding a protein V that was unable to bind NPM1. For HPV16, we demonstrate a transient association of NPM1 with L2 that is resolved early in the assembly process. However, this early interaction between L2 and NPM1 is not required for production of grossly normal capsids, but instead it promotes subtle alterations in the conformations of L2 and L1 in the assembled capsids. We provide strong evidence that the L2 in defective PsV produced in the presence of reduced NPM1 levels prematurely releases from the capsid at early time points during infection, which abrogates its ability to mediate the nuclear delivery of the viral genome necessary for successful infection.

Acknowledgments

We thank Carla Cerqueira for providing the HPV16 C428S pentamers and Xin Wei Wang (NCI, NIH) for providing the NPM1 expression plasmid. This research was supported by the Intramural Research Program of the National Institutes of Health, through project ZIABC009052 of the Center for Cancer Research, NCI, NIH.

Appendix A. Supporting information

Supplementary data associated with this article can be found in the online version at http://dx.doi.org/10.1016/j.pvr.2015.06.005.

References

[1] P.M. Howley, D.R. Lowy, Papillomaviruses, Fields Virology, Lippincott Williams & Wilkins, Philadelphia (2013) 1662–1703.
[2] C.B. Buck, D.V. Pastrana, D.R. Lowy, J.T. Schiller, Efficient intracellular assembly of papillomaviral vectors, J. Virol. 78 (2004) 751–757.
[3] C.B. Buck, N. Cheng, C.D. Thompson, D.R. Lowy, A.C. Steven, J.T. Schiller, et al., Arrangement of L2 within the papillomavirus capsid, J. Virol. 82 (2008) 5190–5197.
[4] M. Sapp, M. Bienkowska-Haba, Viral entry mechanisms: human papillomavirus and a long journey from extracellular matrix to the nucleus, FEBS J. 276 (2009) 7206–7216.
[5] P.M. Day, M. Schelhaas, Concepts of papillomavirus entry into host cells, Curr. Opin. Virol. 4 (2014) 24–31.
[6] R. Kirnbauer, F. Booy, N. Cheng, D.R. Lowy, J.T. Schiller, Papillomavirus L1 major capsid protein self-assembles into virus-like particles that are highly immunogenic, Proc. Natl. Acad. Sci. USA 89 (1992) 12180–12184.
[7] D.R. Lowy, J.T. Schiller, Prophylactic human papillomavirus vaccines, J. Clin. Investig. 116 (2006) 1167–1173.
[8] P.M. Day, R.B. Roden, D.R. Lowy, J.T. Schiller, The papillomavirus minor capsid protein, L2, induces localization of the major capsid protein, L1, and the viral transcription/replication protein, E2, to PML oncogenic domains, J. Virol. 72 (1998) 142–150.
[9] T. Nakahara, P.F. Lambert, Induction of promyelocytic leukemia (PML) oncogenic domains (PODs) by papillomavirus, Virology 366 (2007) 316–329.
[10] P.M. Day, C.C. Baker, D.R. Lowy, J.T. Schiller, Establishment of papillomavirus infection is enhanced by promyelocytic leukemia protein (PML) expression, Proc. Natl. Acad. Sci. USA 101 (2004) 14252–14257.
[11] P.M. Day, C.D. Thompson, R.M. Schowalter, D.R. Lowy, J.T. Schiller, Identification of a role for the trans-Golgi network in human papillomavirus 16 pseudovirus infection, J. Virol. 87 (2013) 3862–3870.
[12] A. Lipovsky, A. Popa, G. Pimienta, M. Wyler, A. Bhan, L. Kuruvilla, et al., Genome-wide siRNA screen identifies the retromer as a cellular entry factor for human papillomavirus, Proc. Natl. Acad. Sci. USA 110 (2013) 7452–7457.
[13] M. Okuwaki, The structure and functions of NPM1/Nucleophsmin/B23, a multifunctional nucleolar acidic protein, J. Biochem. 143 (2008) 441–448.
[14] R.B. Roden, H.L. Greenstone, R. Kirnbauer, F.P. Booy, J. Jessie, D.R. Lowy, et al., In vitro generation and type-specific neutralization of a human papillomavirus type 16 virion pseudotype, J. Virol. 70 (1996) 5875–5883.
[15] K.M. Johnson, R.C. Kines, J.N. Roberts, D.R. Lowy, J.T. Schiller, P.M. Day, Role of heparan sulfate in attachment to and infection of the murine female genital tract by human papillomavirus, J. Virol. 83 (2009) 2067–2074.
[16] D.V. Pastrana, R. Gambhira, C.B. Buck, Y.Y. Pang, C.D. Thompson, T.D. Culp, et al., Cross-neutralization of cutaneous and mucosal Papillomavirus types with anti-sera to the amino terminus of L2, Virology 337 (2) (2005) 365–372.
[17] P.M. Day, Y.Y. Pang, R.C. Kines, C.D. Thompson, D.R. Lowy, J.T. Schiller, A human papillomavirus (HPV) in vitro neutralization assay that recapitulates the in vitro process of infection provides a sensitive measure of HPV L2 infection-inhibiting antibodies, Clin. Vaccine Immunol.: CVI 19 (2012) 1075–1082.
[18] R. Gambhira, B. Karanam, S. Jagu, J.N. Roberts, C.B. Buck, I. Bossis, et al., A protective and broadly cross-neutralizing epitope of human papillomavirus L2, J. Virol. 81 (2007) 13927–13931.
[19] I. Rubio, H. Seitz, E. Canali, P. Sehr, A. Bolchi, M. Tommasino, et al., The N-terminal region of the human papillomavirus L2 protein contains overlapping binding sites for neutralizing, cross-neutralizing and non-neutralizing antibodies, Virology 409 (2011) 348–359.
[20] J.W. Chen, T.L. Murphy, M.C. Willingham, I. Pastan, J.T. August, Identification of two lysosomal membrane glycoproteins, J. Cell Biol. 101 (1985) 85–95.
[21] W. Wang, A. Budhu, M. Forgues, X.W. Wang, Temporal and spatial control of nucleophosmin by the Ran-Crm1 complex in centrosome duplication, Nat. Cell Biol. 7 (2005) 823–830.
[22] R.G. Verhaak, C.S. Goudswaard, W. van Putten, M.A. Bijl, M.A. Sanders, W. Hugens, et al., Mutations in nucleophosmin (NPM1) in acute myeloid leukemia (AML): association with other gene abnormalities and previously established gene expression signatures and their favorable prognostic significance, Blood 106 (2005) 3747–3754.
[23] G. Cardone, A.L. Moyer, N. Cheng, C.D. Thompson, I. Dvoretzky, D.R. Lowy, et al., Maturation of the human papillomavirus 16 capsid, mBio 5 (2014) e01104–e01114.
[24] P.M. Day, C.D. Thompson, C.B. Buck, Y.Y. Pang, D.R. Lowy, J.T. Schiller, Neutralization of human papillomavirus with monoclonal antibodies reveals different mechanisms of inhibition, J. Virol. 81 (2007) 8784–8792.
[25] P.M. Day, R. Gambhira, R.B. Roden, D.R. Lowy, J.T. Schiller, Mechanisms of human papillomavirus type 16 neutralization by l2 cross-neutralizing and l1 type-specific antibodies, J. Virol. 82 (2008) 4638–4646.
[26] M. Staufenbiel, W. Deppert, Preparation of nuclear matrices from cultured cells: subfractionation of nuclei in situ, J. Cell Biol. 98 (1984) 1886–1894.
[27] A. Handisurya, P.M. Day, C.D. Thompson, C.B. Buck, Y.Y. Pang, D.R. Lowy, et al., Characterization of Mus musculus papillomavirus 1 infection in situ reveals an unusual pattern of late gene expression and capsid protein localization, J. Virol. 87 (2013) 13214–13225.
[28] T.D. Culp, N.M. Cladel, K.K. Balogh, L.R. Budgeon, A.F. Mejia, N.D. Christensen, Papillomavirus particles assembled in 293TT cells are infectious in vivo, J. Virol. 80 (2006) 11381–11384.
[29] L. Florin, C. Sapp, R.E. Streeck, M. Sapp, Assembly and translocation of papillomavirus capsid proteins, J. Virol. 76 (2002) 10009–10014.
[30] L. Florin, F. Schafer, K. Sotlar, R.E. Streeck, M. Sapp, Reorganization of nuclear domain 10 induced by papillomavirus capsid protein l2, Virology 295 (2002) 97–107.

[31] E. Kieback, M. Muller, Factors influencing subcellular localization of the human papillomavirus L2 minor structural protein, Virology 345 (2006) 199–208.
[32] H. Ugai, G.C. Dobbins, M. Wang, L.P. Le, D.A. Matthews, D.T. Curiel, Adenoviral protein V promotes a process of viral assembly through nucleophosmin 1, Virology 432 (2012) 283–295.
[33] R.A. Borer, C.F. Lehner, H.M. Eppenberger, E.A. Nigg, Major nucleolar proteins shuttle between nucleus and cytoplasm, Cell 56 (1989) 379–390.
[34] S. Grisendi, R. Bernardi, M. Rossi, K. Cheng, L. Khandker, K. Manova, et al., Role of nucleophosmin in embryonic development and tumorigenesis, Nature 437 (2005) 147–153.
[35] S. Chiarella, A. De Cola, G.L. Scaglione, E. Carletti, V. Graziano, D. Barcaroli, et al., Nucleophosmin mutations alter its nucleolar localization by impairing G-quadruplex binding at ribosomal DNA, Nucl. Acids Res. 41 (2013) 3228–3239.
[36] B. Falini, N. Bolli, J. Shan, M.P. Martelli, A. Liso, A. Pucciarini, et al., Both carboxy-terminus NES motif and mutated tryptophan(s) are crucial for aberrant nuclear export of nucleophosmin leukemic mutants in NPMc+ AML, Blood 107 (2006) 4514–4523.
[37] B. Falini, I. Nicoletti, N. Bolli, M.P. Martelli, A. Liso, P. Gorello, et al., Translocations and mutations involving the nucleophosmin (NPM1) gene in lymphomas and leukemias, Haematologica 92 (2007) 519–532.
[38] C.B. Buck, C.D. Thompson, Y.-Y.S. Pang, D.R. Lowy, J.T. Schiller, Maturation of papillomavirus capsids, J. Virol. 79 (5) (2005) 2839–2846.
[39] R.M. Richards, D.R. Lowy, J.T. Schiller, P.M. Day, Cleavage of the papillomavirus minor capsid protein, L2, at a furin consensus site is necessary for infection, Proc. Natl. Acad. Sci. USA 103 (2006) 1522–1527.
[40] R.C. Kines, C.D. Thompson, D.R. Lowy, J.T. Schiller, P.M. Day, The initial steps leading to papillomavirus infection occur on the basement membrane prior to cell surface binding, Proc. Natl. Acad. Sci. USA 106 (2009) 20458–20463.
[41] J.W. Wang, R.B. Roden, L2, the minor capsid protein of papillomavirus, Virology 445 (2013) 175–186.
[42] L. Florin, K.A. Becker, C. Sapp, C. Lambert, H. Sirma, M. Muller, et al., Nuclear translocation of papillomavirus minor capsid protein l2 requires hsc70, J. Virol. 78 (2004) 5546–5553.
[43] M.B. Marusic, N. Mencin, M. Licen, L. Banks, H.S. Grm, Modification of human papillomavirus minor capsid protein L2 by sumoylation, J. Virol. 84 (2010) 11585–11589.
[44] M. Carmo-Fonseca, L. Mendes-Soares, I. Campos, To be or not to be in the nucleolus, Nat. Cell Biol. 2 (2000) E107–E112.
[45] M.O. Olson, M. Dundr, A. Szebeni, The nucleolus: an old factory with unexpected capabilities, Trends Cell Biol. 10 (2000) 189–196.
[46] P. Banski, M. Kodiha, U. Stochaj, Chaperones and multitasking proteins in the nucleolus: networking together for survival? Trends Biochem. Sci. 35 (2010) 361–367.
[47] M. Bienkowska-Haba, H.D. Patel, M. Sapp, Target cell cyclophilins facilitate human papillomavirus type 16 infection, PLoS Pathog. 5 (2009) e1000524.
[48] P.K. Chan, F.Y. Chan, Nucleophosmin/B23 (NPM) oligomer is a major and stable entity in HeLa cells, Biochim. Biophys. Acta 1262 (1995) 37–42.
[49] C.D. Liu, Y.L. Chen, Y.L. Min, B. Zhao, C.P. Cheng, M.S. Kang, et al., The nuclear chaperone nucleophosmin escorts an Epstein-Barr Virus nuclear antigen to establish transcriptional cascades for latent infection in human B cells, PLoS Pathog. 8 (2012) e1003084.
[50] Y. Tsuda, Y. Mori, T. Abe, T. Yamashita, T. Okamoto, T. Ichimura, et al., Nucleolar protein B23 interacts with Japanese encephalitis virus core protein and participates in viral replication, Microbiol. Immunol. 50 (2006) 225–234.
[51] Z. Duan, J. Chen, H. Xu, J. Zhu, Q. Li, L. He, et al., The nucleolar phosphoprotein B23 targets Newcastle disease virus matrix protein to the nucleoli and facilitates viral replication, Virology 452–453 (2014) 212–222.
[52] F. Sonntag, K. Schmidt, J.A. Kleinschmidt, A viral assembly factor promotes AAV2 capsid formation in the nucleolus, Proc. Natl. Acad. Sci. USA 107 (2010) 10220–10225.